Study on Turbulent Boundary Layer with Injection and Combustion

By

Mamoru SENDA*, Kenjiro SUZUKI* and Takashi SATO*

(Received September 30, 1975)

Abstract

Results are presented of the calculation of the velocity field and of the experiments of mean profile measurements in the turbulent boundary layer with injection and combustion. The agreement between the present calculation, which is the extension of the Economos' method, and the experimental results of other investigators is not very good. Thus, the cause of this disagreement is discussed by making use of the results of the present measurements. Through further examination of the same experimental results, some characteristics of the flow are clarified, and the important points to be considered during future study are pointed out.

Nomenclature

$B, \bar{B}$: $2F/c_f, 2\bar{F}/\bar{c}_f$

$c_f, \bar{c}_f$:   local skin friction coefficients

$F, \bar{F}$: $(\rho v)_w/(\rho u)_e, (\bar{\rho}\bar{v})_w/(\bar{\rho}\bar{u})_e$

$R_x, R_{\bar{x}}$:   Reynolds number based on $x, \bar{x}$

$R_y, R_{\bar{y}}$:   Reynolds number based on $y, \bar{y}$

$R_\delta, R_{\bar{\delta}}$:   Reynolds number based on $\delta, \bar{\delta}$

$R_\theta, R_{\bar{\theta}}$:   Reynolds number based on $\theta, \bar{\theta}$

$u, \bar{u}$:   streamwise velocity components

$v, \bar{v}$:   normal velocity components

$x, \bar{x}$:   streamwise coordinates

$y, \bar{y}$:   normal coordinates

$\delta, \bar{\delta}$:   boundary layer thickness

ξ, η, σ: parameters of the transformation

$\theta, \bar{\theta}$:   momentum thickness

* Department of Mechanical Engineering

$\mu, \bar{\mu}$:   viscosities

$\rho, \bar{\rho}$:   densities

$\tau, \bar{\tau}$:   shear stresses

$\psi, \bar{\psi}$:   stream functions

Subscripts

e :   external conditions

s :   sublayer edge conditions

w :   wall conditions

1. Introduction

Boundary layers with injection and combustion are encountered in the flow environments of the hybrid rocket engine and the high speed re-entry body.   Because of high Reynolds number and low critical Reynolds number due to injection, the boundary layers are likely to be turbulent in these flow environments.   Therefore, it is important to get the comprehensive ideas of momentum, heat and mass transfer processes in the turbulent boundary layer with injection and combustion.   However, there are only a few fundamental investigations.

Wooldridge et al.[1] measured the mean profiles and some turbulent properties, using a mixture of hydrogen and nitrogen as the injected fuel.   Jones et al.[2] investigated the interaction between the combustion process and the velocity field, both experimentally and analytically, using the same injected fuel as that of Wooldridge et al. However, there was a difference between their results and those of Wooldridge et al. Kulgein[3] also measured the mean profiles from a viewpoint of the analogy of momentum, heat and mass transfer processes, but used methane as the injected fuel.   The value of the skin friction coefficient for small injection rate was even higher than that of the case without injection, in contrast to the results obtained by Jones et al. and Wooldridge et al.

The purpose of this study is to investigate the heat transfer mechanism of turbulent boundary layer with injection and combustion.   This report is concerned with a first stage study of the project, involving the analytical study with a modified Economos' procedure of the form applicable to the present problem, and the experimental study on the profiles of velocity, temperature and concentration of some important species.

2. Calculation and Discussion

The calculation presented here is based on the Economos' theory, so that the essential part of the method can be found in his papers.[4],[5]   For an easy understanding of the modified points, however, it is briefly traced at first.   In this chapter, the outline

of the calculation is presented and the details are summarized in the appendix.

The main concept of this theory is a compressibility transformation, relating a variable property flowfield of interest to a companion constant property flowfield. After the Economos' example, the flowfield of interest characterized by the variable properties is called the VP flow and the related one characterized by the constant properties is called the CP flow.

In considering the steady, two-dimensional turbulent flow without pressure gradient, where the fluid properties are variable (VP flow), the governing equations for the velocity field are written in the following forms

$$\frac{\partial(\rho u)}{\partial x} + \frac{\partial(\rho v)}{\partial y} = 0 \tag{1}$$

$$\rho u \frac{\partial u}{\partial x} + \rho v \frac{\partial u}{\partial y} = \frac{\partial \tau}{\partial y} \tag{2}$$

It can be shown that this flowfield can be transformed into the companion flowfield, where the fluid properties are constant (CP flow), by introducing the following transformation relations:

$$d\bar{x}/dx = \xi(x) \tag{3}$$

$$\bar{\rho} d\bar{y}/\rho dy = \eta(x) \tag{4}$$

$$(\bar{\psi} - \bar{\psi}_w)/(\psi - \psi_w) = \sigma(x) \tag{5}$$

and the governing equations of the CP flow are as follows

$$\frac{\partial \bar{u}}{\partial \bar{x}} + \frac{\partial \bar{v}}{\partial \bar{y}} = 0 \tag{6}$$

$$\bar{\rho} \bar{u} \frac{\partial \bar{u}}{\partial \bar{x}} + \bar{\rho} \bar{v} \frac{\partial \bar{u}}{\partial \bar{y}} = \frac{\partial \bar{\tau}}{\partial \bar{y}} \tag{7}$$

Here, the CP flow variables are distinguished by (¯) from those of the VP flow.

The correspondences between gross boundary layer parameters of the two flowfields can be derived by using the above transformation relations. The calculation is carried out with these correspondences, and the momentum integral equations of the two flowfields. For the implementation of this theory, it is necessary to know the suitable CP flow characteristics. In the present calculation, the results obtained by Stevenson[6],[7] are utilized for this purpose.

All of the relations necessary for the calculation have already been prepared. The remaining problem is to relate the density and the viscosity in the VP flow to the velocity, as seen from Eq. (A4) in the appendix. In place of solving the energy and species concentration equations of the VP flow simultaneously, it is assumed that the thermodynamics of the VP flow can be related to the velocity field. For this

purpose, the following assumptions are adopted:

(1) Molecular and turbulent Prandtl and Schmidt numbers are equal to unity, respectively.

(2) Chemical reaction rate is infinite, or combustion takes place in an infinitesimally thin flame sheet.

Some modifications are given to the original Economos' method in connection with the second assumption. The enthalpy and the mass fraction profiles are linearly related to the velocity profile with these assumptions even in the case with combustion.

The first assumption makes the relation between enthalpy (or mass fraction) and velocity easy to be dealt with. Incidentally, this assumption can be replaced without any difficulty by the alternative assumption that the Lewis number is equal to unity, if the thin film theory is used for the viscous sublayer. However, the results are not improved noticeably by this replacement. Accordingly, only the calculation with the former assumption is set forth below.

The outline of the calculation procedure is as follows. Firstly, the gross boundary layer parameters in the CP flow are obtained as a function of Reynolds number for a given blowing parameter B in the VP flow, and the velocity field in the CP flow are determined completely. Then, the gross boundary layer parameters in the VP flow are obtained by using the correspondence relations between the two flowfields. As $u/u_e = \bar{u}/\bar{u}_e$ from Eq. (A1) in the appendix, the calculation of the velocity profile in the VP flow can be performed by transforming the normal coordinate $\bar{y}$ into y with Eq. (4).

In order to compare with the experimental results of Wooldridge *et al.* and Jones *et al.*, the present calculation is carried out for the injection of hydrogen-nitrogen mixture. The results of the calculation with the above procedure are shown and compared with their experimental results in Fig. 1 and 2. The present calculation
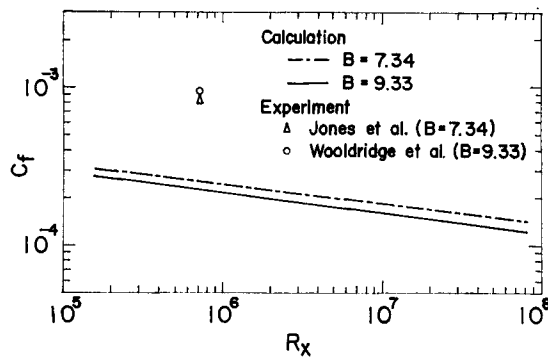

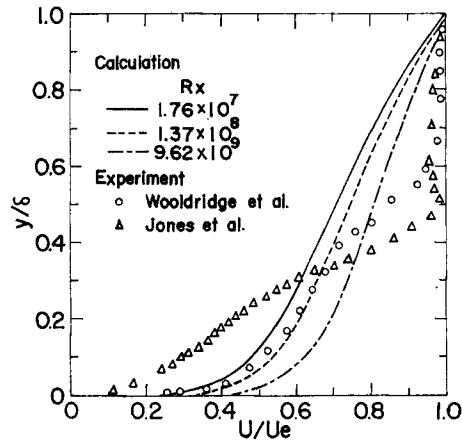Fig. 1. Comparison of the calculation and the experiments
—Skin friction coefficient—

Fig. 2. Comparison of the calculation and the experiments —Velocity profile—

does not agree with either of their results. The disagreement between the present calculation and the experimental results can possibly be ascribed to the adoption of a thin flame sheet model. This is because the fluid density near the flame region is estimated to be too high as the result of the adoption of the model. Then, the velocity profile in the VP flow is much affected by the density profile in connection with the coordinate transformation relationship Eq. (4). The fact that the combustion zone has a finite thickness will be shown later. Jones *et al.,* whose results are to be shown in Fig. 9, used in their analysis the profiles of the measured temperature and species concentration for the evaluation of the fluid density. These profiles, however, are not available a priori in practical problems, so that some more refined combustion model must be invented to develop the present theory or one similar to this.

On the other hand, the finite chemical reaction rate has been taken into account[8] by utilizing a numerical prediction technique, employing the same turbulence model as that of Jones *et al.* This model consists of the mixing length theory modified with the van Driest's damping factor in the region near the wall and the Klebanoff's relation accounting for the intermittency in the outer region. The calculated velocity profile, as well as that of Jones *et al.,* has a remarkable inflection point near the combustion zone, which is clearly seen in the experimental results in the above figure. The present calculation, however, does not show such a characteristic feature remarkably. Such a comparison seems to suggest that only a refinement of the combustion model can promise the success of calculation even with the present procedure. Before concluding this, however, it might be worthwhile to discuss the turbulence model employed in each procedure.

The advantage of the present compressibility transformation theory resides in the fact that there is no need to express the shear stress in the VP flow explicitly. This

means, however, that the local shear stress used implicitly is no more than a reflection
of the one adopted in the CP flow, namely, of the mixing length theory on which
Stevenson's results are based. Thus, it can be said that even the effect of injection
on the turbulence structure is not taken into account. In contrast with this, the other
two analyses consider the injection effect. In this point, these calculations are superior
to the present one.

In the present flow, however, it is natural to consider that the turbulence structure
is changed due to the interaction with combustion. In fact, Eschenroeder[9] pointed
out that the turbulence is amplified by heat release and the experiments of Wooldridge
et al.[10] support his suggestion. All the calculations being discussed now are the
same, in the sense that they did not account for the possible amplification of the
turbulence, and took into account only the so called kinematic effects on the turbulence
structure. If the effects, both of injection and interaction with combustion, are not
essential, success may be expected even with the present theory only by the refinement
of the combustion model. What can be said at present, however, is that the conside-
ration of the combustion effect on the turbulence structure is necessary as well as of
a more refined combustion model.

In connection with the above argument, it must be noticed that the experimental
velocity profiles of Wooldridge et al. and of Jones et al. are very different in forms
from each other, although their experimental conditions are almost the same. As
discussed later, an error might be involved in the experiments of the velocity profiles
with the pitot static tube. If there had been no doubt about the correctness of these
experimental results, the theoretical side of the present works would have been developed
much further.

3. Experimental Apparatus and Procedure

A schematic diagram of the experimental apparatus is given in Fig. 3. The
test section is 300 mm by 300 mm in cross section and 1800 mm in length. An up-
stream end of the test section is a sharp leading edge of an angle 3°. At this leading
edge, the boundary layer developed ahead of the test section is sucked so that a new
boundary layer develops from there. The distance from this leading edge to the
section of porous plates is 600 mm, and the porous plates section inserted in the lower
wall consists of five 180 mm by 180 mm porous plates. The porous plates are made
from grindstone with the porosity being about 40%. All the experiments are carried
out with the uniform blowing rate F over the whole injection area.

The test section has a movable upper wall and 17 static pressure taps are provided
on the side wall. Prior to the experiments, the upper wall is carefully adjusted to
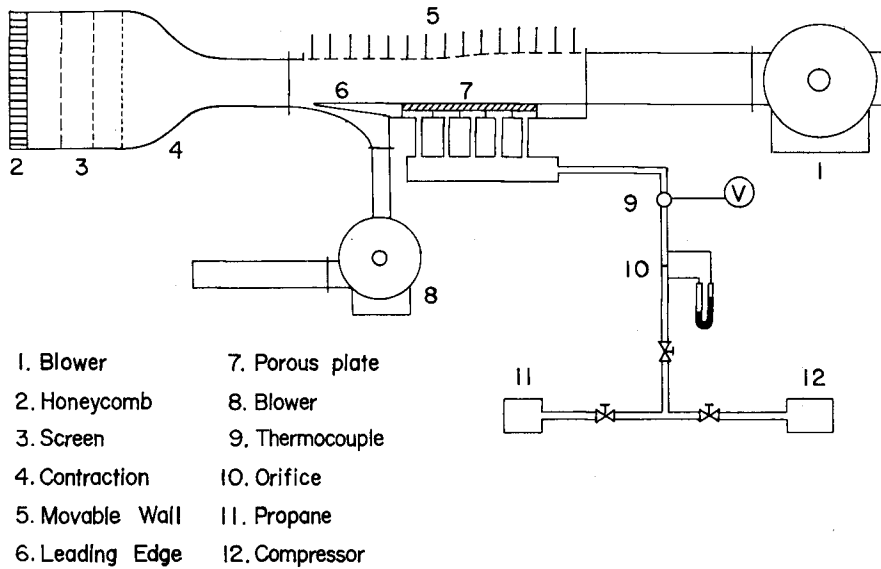minimize the static pressure variation along the streamwise direction. The variation

1. Blower   7. Porous plate
2. Honeycomb   8. Blower
3. Screen   9. Thermocouple
4. Contraction   10. Orifice
5. Movable Wall   11. Propane
6. Leading Edge   12. Compressor

Fig. 3. Schematic diagram of the experimental apparatus

of the static pressure relative to the dynamic pressure along the porous plates section is around $\pm 1.0\%$, at most.

For the non-combustion experiments, air supplied by the compressor is injected into the boundary layer, whereas in the combustion experiments propane gas is used as the injected fuel. After ignition, the diffusion flame of propane is formed within the boundary layer.

Measurements of the dynamic pressure are carried out with the pitot tube consisting of the total pressure and static pressure tubes. These tubes are made of a stainless steel tube having 0.8 mm inner diameter and 1.0 mm outer diameter. They are placed in the same horizontal plane, but are spaced laterally to avoid mutual interference. The temperature profiles in the boundary layer are measured with $50\,\mu$-diameter Pt·Rd (30%)–Pt·Rd (6%) thermocouple. The correction for radiation loss is not made. For the determination of concentration profiles, sample gas is extracted through a sampling probe made of the same stainless steel tube as the total pressure tube and is analyzed with a gas chromatograph. The extracting speed of the sample gas is adjusted so to be the same as the local velocity in the boundary layer. Before analyzing the sample gas, H_2O is removed by passing the sample gas through the glass tube packed with $CaCl_2$ and, therefore, the concentration profile of H_2O is not available in this report.

4. Results and Discussion of the Experiments

Velocity profiles without injection are shown in Fig. 4. The friction velocity, u_τ, was determined from the well-known empirical relations; $\delta=0.37x(u_e x/\nu)^{-0.2}$ and $c_f/2=0.0296(u_e x/\nu)^{-0.2}$. Here, x_p denotes the distance from the leading edge of the porous plates.

In Fig. 5, velocity profiles with injection are shown and compared with the Stevenson's analytical results. The ordinate Φ is $\Phi=\sqrt{2c_f/F}[(1+B)^{1/2}-(1+Bu/u_e)^{1/2}]$. c_f was determined from the Kays'[11] empirical relation; $c_f/2=0.013\,R_\theta^{-1/4}[\ln(1+B)/B]^{0.77}$. Reynolds number based on the momentum thickness R_θ was calculated from the measured velocity profiles. The agreement with Stevenson's results is not very good. The cause of this is suspected to be the fact that the boundary layer with
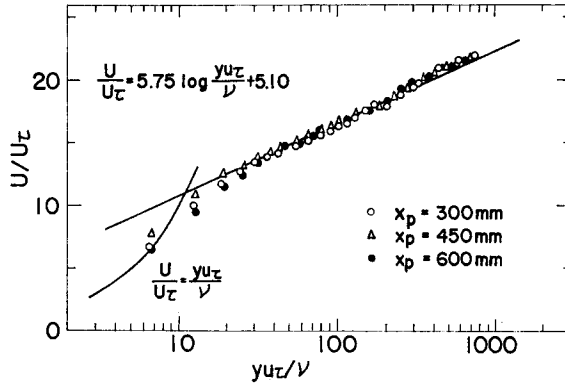
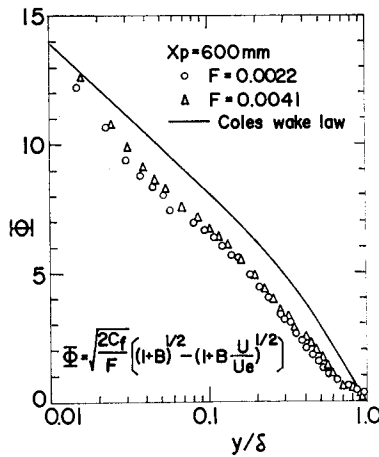Fig. 4.   Velocity profiles without injection

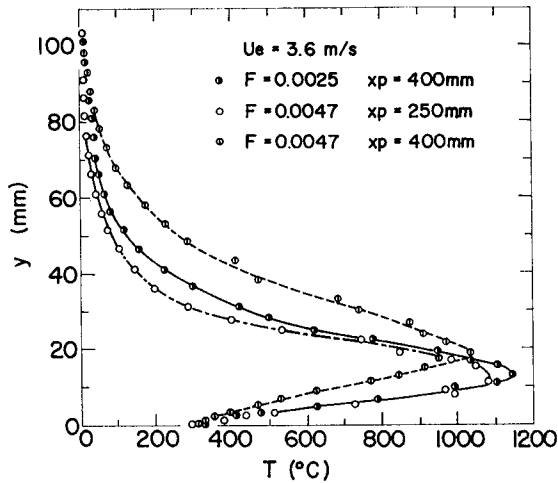Fig. 5.   Velocity profiles with injection

Fig. 6. Temperature profiles with combustion

injection was not yet reached to be the equilibrium condition. This is partly due either to a little thick boundary layer, or to a short porous plates section. The stable flame could not be obtained at a higher Reynolds number. The experiments at a higher Reynolds number ensuring equilibrium state will be the subject in future. The primary intention of the present experiments is to compare the results with those of Wooldridge *et al.* and Jones *et al.,* obtained with the apparatus of almost the same dimensions as the present one, except the injected fuel.

The temperature profiles with injection and combustion are shown in Fig. 6. The profiles exhibit a definite roundness about their maximum point, indicating that the chemical reaction occurs over a small, but finite thickness region rather than in an infinitesimally thin sheet. This is the same result as that of Wooldridge *et al.* This roundness becomes more remarkable with the distance and, at the same time, the maximum temperature becomes lower. Both facts indicate the thickening of the flame-zone with the distance. The position of the maximum temperature moves towards the boundary layer edge with the distance, too, and this phenomenon matches the increase of the similarity parameter $B(=F/St)$ with the distance. (St is Stanton number)

In Fig. 7 are shown the concentration profiles. From these experimental results, several characteristics can be found for the turbulent boundary layer with combustion. Firstly, there exist regions where both the fuel (propane) and the oxidizer (oxygen) are present. Both species are spread over the maximum temperature point, extending to the wall side (oxidizer) and the free boundary side (fuel). Secondly, there exist several intermediate products besides the reactants and the products. The existence
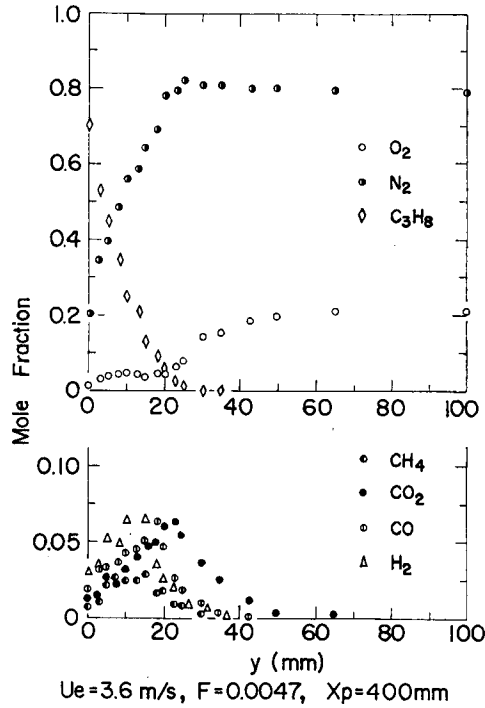
Fig. 7.   Species concentration profiles with combustion

of these intermediate products indicates that the reaction is not a one-step reaction, but seems to be a more complicated form.   From the figure, it can also be seen that the maximum positions of CH_4, CO, and H_2 profiles are almost the same.   Moreover, they are different from that of CO_2 and are nearer to the wall.   Thirdly, the maximum position of CO_2 and that of temperature are almost the same.   All the facts mentioned above also suggest the finite reaction zone, rather than the infinitesimally thin flame sheet as assumed in the calculation mentioned previously.

According to the preliminary evaluation, it was found that the density of gas mixture was not affected very much by the local change in concentration of each species except very near the wall.   For that reason, the local density of gas mixture was calculated only by taking into consideration the temperature of that position, and was used for the calculation of the velocity from the measured dynamic pressure profile.

The velocity profiles with combustion are shown in Fig. 8.   Each velocity profile has a maximum within the boundary layer, i.e. there is a region where the local velocity in the boundary layer exceeds the freestream velocity.   This maximum point of velocity is in the very vicinity of the reaction zone.   This is also the same tendency as shown in the results of Jones *et al.*
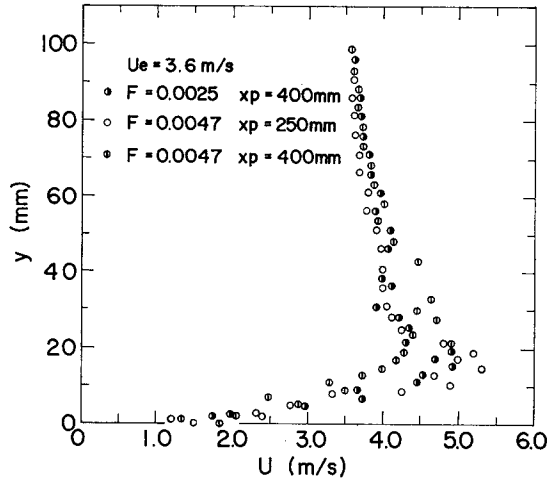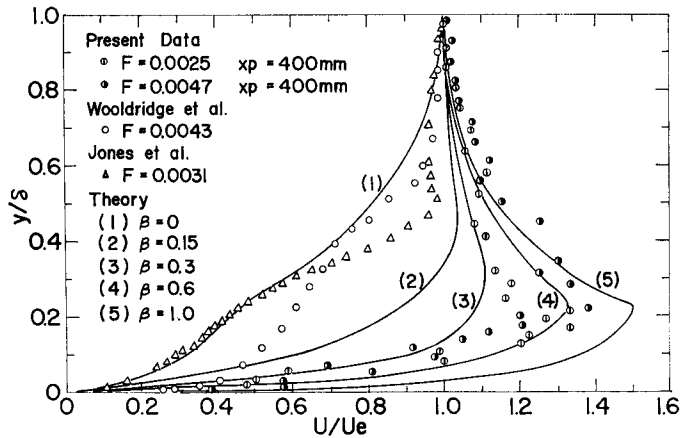
Fig. 8. Velocity profiles with combustion

Fig. 9. Comparison of the experimental velocity profiles and the analysis
of Jones *et al.*

In the boundary layer with combustion, there exists a high temperature region, and the flowfield becomes much more sensitive to the pressure gradient as a result of the small local mean density near the flame zone. Consequently, there is a possibility that this velocity overshoot occurs because of a rather small pressure gradient left unremoved. Jones *et al.* investigated this phenomenon analytically and experimentally and showed that the velocity maxima result from the pressure gradient. In Fig. 9, the present results are compared with the calculated profiles of Jones *et al.* Here, β is a wedge parameter and is defined as $\beta=(2\xi/u_e)\,du_e/d\xi$ and $\xi=\int_0^x \rho_e u_e \mu_e dx$.

As mentioned previously, the ratio of static pressure variation to the dynamic

pressure in these experiments was within $\pm 1.0\%$, and the wedge parameter β calculated from the small systematic variation of static pressure left unremoved all over the whole test section was, at most, 0.05.   The remarkable velocity overshoot shown in the present experiments can not be expected at this low value of β, according to the analysis of Jones *et al*.   There might be a possibility that the local pressure gradient in connection with the above level of unordered static pressure scattering was a cause of velocity overshoot.   This, however, does not seem to be the only possible explanation.   In particular, it may be important to note that the velocity profiles obtained at two different cross-sections have the velocity maxima of almost the same level, and that such phenomenon may not be explained only from the view point of the local static pressure gradient.

On the other hand, the turbulence intensity of the present type of flow is much higher than that found in an ordinary type of turbulent boundary layer.[10]   Moreover, the density fluctuation is expected to exist, and the correlation between the density and the velocity fluctuations becomes important to some extent.   Consequently, it may not be so strange to think that this velocity overshoot might be partly brought about by the effect of turbulent fluctuation on the reading of the pitot tube.   In order to examine the cause of velocity maxima more definitely, anyway, it is necessary to lower the level of the pressure gradient still more, and to investigate carefully the effect of turbulent fluctuation on the dynamic pressure.

Another characteristic feature seen in the figure is the gentle velocity gradient near the wall.   This characteristic is also seen in the results of Wooldridge *et al*. and is shown in the same figure.   This gentle slpoe of velocity can be considered to be the consequence of the increase of the kinematic viscosity due to a high temperature. While the lowering of the critical Reynolds number occurs because of injection as well as the increase of eddy viscosity by the amplification of turbulence due to combustion in this flowfield, the effect of the lowered Reynolds number seems to be more effective near the wall.

Lastly, the differences between the results of Wooldridge *et al*. and those of Jones *et al*. are yet of unknown origin, and this is a remaining problem to be considered in the future.

5. Concluding Remarks

In the first place, the Economos' method was extended to a form applicable for turbulent boundary layer with injection and combustion.   There was a great difference between the prediction with the modified Economos' method and the experiments. The main cause of the disagreement was considered to reside in the infinitesimally thin flame sheet model for combustion, adopted in the analysis.

At the same time, measurements of the temperature, concentration and velocity profiles were performed in the combustion experiments. The following characteristics were clarified through the temperature and concentration measurements. Firstly, the temperature profiles in the boundary layer exhibit a definite roundness about their maximum point. Secondly, the species concentration profiles indicate that there exist some finite concentrations of oxidizer and fuel below and above the flame, respectively. Thirdly, propane is decomposed into simpler hydro-carbons and the chemical reaction is not so simple one as the one-step reaction. These experimental results indicate the existence of the finite thickness reaction zone rather than the thin flame sheet. Consequently, the development of the theory in which the finite thickness reaction zone is taken into consideration is necessary.

However, injection and combustion may change the turbulence structure as suggested by Eschenroeder and supported by the experiments of Wooldridge *et al*. Accordingly, it is insufficient only to consider the finite chemical reaction rate in the conservation equations in order to take account of the finite thickness reaction zone. It is also necessary to consider the change of the turbulence structure simultaneously.

Turbulence models which can be applied to the flow with combustion have been rarely found and should be devised by refering to some models developed for a much simpler flowfield. For this purpose, careful experiments on turbulence are still necessary in a little simpler turbulent boundary layer, for example, isothermal and non-isothermal ones with injection or a turbulent boundary layer with foreign gas injection, as well as in the present one. These are important not only for the foundation of the turbulence model of the flow with combustion, but also, of course, for other engineering problems.

Finally, the velocity profiles exhibit the overshoot in the vicinity of the reaction zone. Two possible explanations for this are the effect of local pressure gradient and the effect of turbulent fluctuation on the reading of the pitot tube. Further investigation of the real cause needs experiments under a much lower level of static pressure gradient and the careful study of the latter.

Appendix

The correspondences between gross boundary layer parameters of the two flowfields are reduced from Eqs. (3)$\sim$(5) as follows
From definition of stream function:

$$u/\bar{u}=u_e/\bar{u}_e, \quad \text{or} \quad u/u_e=\bar{u}/\bar{u}_e \equiv \tilde{u} \tag{A1}$$

From definition of wall shear stress:

$$c_f/\bar{c}_f=\tilde{\rho}_w\tilde{\mu}_w\tilde{\sigma} \tag{A2}$$

where $\quad \tilde{\rho} \equiv \rho/\rho_e, \quad \tilde{\mu} \equiv \mu/\mu_e \quad$ and $\quad \tilde{\sigma} \equiv \sigma(\mu_e/\bar{\mu})$

From definition of momentum thickness:

$$R_\theta/R_{\bar{\theta}} = 1/\tilde{\sigma} \tag{A3}$$

From definition of coordinate transformation:

$$R_\delta = \left(\frac{1}{\tilde{\sigma}}\right) \int_0^{R_{\bar{\delta}}} \frac{dR_{\bar{y}}}{\tilde{\rho}} \tag{A4}$$

From first wall compatibility condition:

$$\frac{2\bar{F}}{\bar{c}_f} = \frac{2F}{c_f} - \left[\frac{\partial(\tilde{\rho}\tilde{\mu})}{\partial\tilde{u}}\right]_w \tag{A5}$$

From sublayer hypothesis (that is $u_s y_s/\nu_s = \bar{u}_s \bar{y}_s/\bar{\nu}_s$):

$$\tilde{\sigma} = \frac{\tilde{\rho}_s}{\tilde{\mu}_s R_{\bar{y}s}} \int_0^{R_{\bar{y}s}} \frac{dR_{\bar{y}}}{\tilde{\rho}} \tag{A6}$$

From momentum integral equations:

$$\frac{dR_\theta}{dR_x} = F + \frac{c_f}{2}, \qquad \frac{dR_{\bar{\theta}}}{dR_{\bar{x}}} = \bar{F} + \frac{\bar{c}_f}{2} \tag{A7}$$

Following Stevenson, the CP variables are taken to be related by
Velocity profiles:

$$\tilde{u} \equiv \frac{\bar{u}}{\bar{u}_e} = \begin{cases} (2\bar{F}/\bar{c}_f)[\exp(\bar{F}R_{\bar{y}})-1]; & 0 \leq R_{\bar{y}} \leq R_{\bar{y}s} \\ 1 - (\bar{F}+\bar{c}_f/2)^{1/2}\Phi + (\bar{F}/4)\Phi^2; & R_{\bar{y}s} \leq R_{\bar{y}} \leq R_{\bar{\delta}} \end{cases} \tag{A8}$$

Skin friction law:

$$\ln(R_{\bar{\delta}}{}^2\bar{c}_f/2)^{1/2} = K_1\left[\left(\frac{2}{\bar{F}}\right)\left(\frac{\bar{c}_f}{2}\right)^{1/2}\left\{(1+\bar{B})^{1/2}-1\right\} - K_2 - \frac{2\pi}{K_1}\right] \tag{A9}$$

Momentum thickness:

$$\frac{R_{\bar{\theta}}}{R_{\bar{\delta}}} = \left(\frac{\bar{c}_f}{2}\right)^{1/2}(1+\bar{B})^{1/2}\left(I_1 + I_3 \cdot \frac{\bar{F}}{2}\right) - \frac{\bar{c}_f}{2}(1+\bar{B})I_2 - \frac{\bar{F}}{4}\left(I_2 + I_4 \cdot \frac{\bar{F}}{4}\right)$$

$$I_n = \int_0^1 \Phi^n d\left(\frac{\bar{y}}{\bar{\delta}}\right) = I_n(K_1, K_2, \pi) \tag{A10}$$

Sublayer Reynolds number:

$$\exp[(2\bar{F}^2/\bar{c}_f)^{1/2}(R_{\bar{y}s}{}^2\bar{c}_f/2)^{1/2}] - 1 = (\bar{F}^2/2\bar{c}_f)^{1/2}\left[\frac{1}{K_1}\ln(R_{\bar{y}s}{}^2\bar{c}_f/2)^{1/2} + K_2\right] \tag{A11}$$

where Φ and π are the Coles' wake function and the Coles' wake parameter, respectively.
K_1 and K_2 are the usual logarithmic law constants for the impermeable CP flow.

The thermodynamics of the VP flow can be related to the velocity field using the two assumptions adopted in the following way. The enthalpy and the mass fraction profiles are linearly related to the velocity profile with these assumptions. By considering the mass and energy balances both at the wall and at the flame position, the mass fractions of each species and the enthalpies at these boundaries, and the velocity at the flame position can be determined as a function of $B(=2F/c_f)$. For the injection of a hydrogen-nitrogen mixture, the following one-step reaction of hydrogen is assumed:

$$2H_2O + O_2 \rightarrow 2H_2O \tag{A12}$$

The velocity at the flame position can be expressed as:

$$\tilde{u}_c = \frac{u_c}{u_e} = \frac{aB - Y_{O_2e}/\gamma}{B(a + Y_{O_2e}/\gamma)} \tag{A13}$$

where a and γ are the mass fraction of hydrogen in the injected fuel and the O_2-H_2 stoichiometric ratio, respectively. The mass fractions of each species and enthalpies at the wall and the flame position are

$$Y_{H_2w} = \frac{aB}{B + 1/\tilde{u}_c}, \qquad Y_{H_2Ow} = \frac{(1 - \tilde{u}_c)\gamma' Y_{H_2w}}{\tilde{u}_c(1 + B)}$$

$$h_w = \frac{h_e + Bh_{-\infty}}{1 + B}, \qquad Y_{H_2Oc} = \frac{1 - \tilde{u}_c}{Y_{H_2Ow} + \gamma' Y_{H_2w}} \tag{A14}$$

$$h_c = (1 - \tilde{u}_c)h_w + \tilde{u}_c h_e$$

where γ' and $h_{-\infty}$ are the H_2-H_2O stoichiometric ratio and the enthalpy of injectant behind the porous plate, respectively. The density of gas mixture in the VP flow can be written as follows under the assumption of perfect gas:

$$\frac{1}{\tilde{\rho}} = \frac{\rho_e}{\rho} = \left(\frac{T}{T_e}\right)(\sum Y_i/M_i)/(\sum Y_i/M_i)_e \tag{A15}$$

where T is the temperature, and Y_i and M_i are the mass fraction and the molecular weight of i species, respectively. The viscosity of each species is calculated from the rigorous kinetic theory[12], and that of the gas mixture is calculated from the Wilke's equation[12]. The specific heat of each species is taken to be constant, and to have a value of 1000°C.

The calculation procedure is as follows

1) As the density and the viscosity in the VP flow are related to the velocity, the right hand side of Eq. (A5) can be calculated for a given B in the VP flow, and $\bar{B}$ is obtained.

2) With $\bar{B}$, $\bar{c}_f$ can be obtained from Eq. (A7) for a given $R_{\bar{x}}$, and $R_{\bar{\theta}}$ can be calculated from Eqs. (A9) and (A10).

3) When $\bar{c}_f$ is obtained, $\bar{F}$, $R_{\bar{\theta}}$ and $R_{\bar{\delta}}$ are determined from Stevenson's results, and $R_{\bar{y}_s}$ can be calculated from Eq. (A11). Thus, the velocity field in the CP flow are determined completely.

4) Then, $\tilde{\sigma}$ can be calculated from Eq. (A6).

5) With $\tilde{\sigma}$, c_f and R_θ are determined from Eqs. (A2) and (A3). R_x can be calculated from Eq. (A7).

6) As $u/u_e = \bar{u}/\bar{u}_e$, the calculation of the velocity profile in the VP flow can be performed by transforming the normal coordinate $\bar{y}$ into y with Eq. (4). (It can be shown that $\eta/\sigma = u_e/\bar{u}_e$ in the flow without pressure gradient.)

References

1) Wooldridge, C. E. and Muzzy, R. J., 10th Symposium (International) on Combustion, Academic Press, New York, p. 1351 (1965).
2) Jones, J. W., Isaacson, L. K. and Vreeke, S., AIAA J. **9** p. 1762 (1971).
3) Kulgein, N. G., J. Fluid Mech. **12** p. 417 (1962).
4) Economos, C., AIAA J. **8** p. 758 (1970).
5) Economos, C., Ph. D. dissertation, Polytechnie Institute of Brooklyn, (1968).
6) Stevenson, T. N., Rept. 166, College of Aeronautical Research Council of London, England, (1963).
7) Stevenson, T. N., Rept. 20, Aeronautical Research Council of London, England, (1958).
8) Kikkawa, S. and Yoshikawa, K., Trans. Japan Soc. Mech. Engrs., **40** p. 2272 (1974)(in Japanese).
9) Eschenroeder, A. Q., Phys. Fluids. **7** p. 1735 (1964).
10) Wooldridge, C. E. and Muzzy, R. J., AIAA J. **4** p. 2009 (1966).
11) Kays, W. M., Int. J. Heat Mass Transfer **15** p. 1023 (1972).
12) Bird, R. B., Stewart, W. E. and Lightfoot, E. N., "Transport Phenomena" John Wiley & Sons, Inc. (1960).